

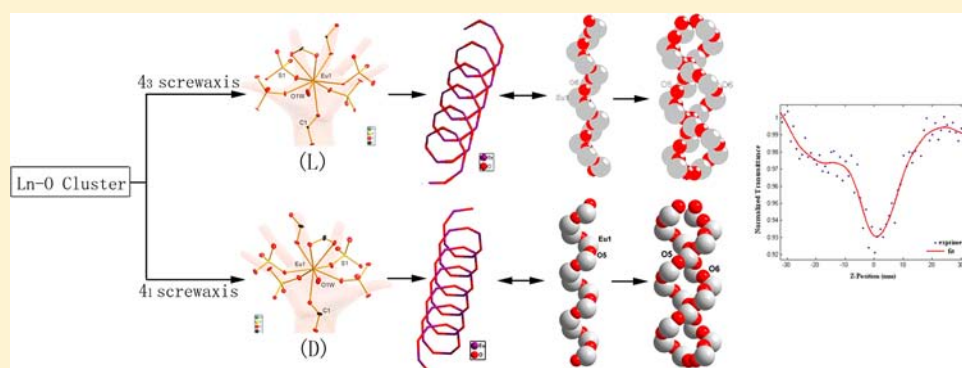
L- and D-[Ln(HCO₂)(SO₄)(H₂O)]_n (Ln = La, Ce, Pr, Nd, and Eu): Chiral Enantiomerically 3D Architectures Constructed by Double –[Ln–O]_n– Helices

Weiwei Ju,[†] Deng Zhang,[†] Dunru Zhu,[†] and Yan Xu^{*,†,‡}

[†]College of Chemistry and Chemical Engineering, State Key Laboratory of Materials-Oriented Chemical Engineering, Nanjing University of Technology, Nanjing 210009, People's Republic of China

[‡]Coordination Chemistry Institute, State Key Laboratory of Coordination Chemistry, Nanjing University, Nanjing 210093, People's Republic of China

S Supporting Information



ABSTRACT: A total of 10 three-dimensional chiral coordination compounds L- and D-[Ln(HCO₂)(SO₄)(H₂O)]_n (Ln = La, Ce, Pr, Nd, and Eu) have been synthesized without any chiral auxiliary and characterized by IR, thermogravimetric, and elemental analyses. Their structures were determined by single-crystal X-ray structural analysis, which shows that L-[Ln(HCO₂)(SO₄)(H₂O)]_n (Ln = La, Ce, Pr, Nd, and Eu) crystallize in space group *P*₄₃ and are laevogyrate and isostructural. The chiral frameworks of L-[Ln(HCO₂)(SO₄)(H₂O)]_n are constructed from L-helical Ln–O cluster chains, while adjacent L-type helical –[Ln–O]_n– chains are connected through O–Ln–O linkages to form chiral intertwined Ln–O double helices of left-handedness. D-[Ln(HCO₂)(SO₄)(H₂O)]_n crystallize in space group *P*₄₁, and their chiral frameworks consist of D-helical Ln–O cluster chains. The observed second-harmonic-generation efficiencies of [La(HCO₂)(SO₄)(H₂O)]_n, [Ce(HCO₂)(SO₄)(H₂O)]_n, [Pr(HCO₂)(SO₄)(H₂O)]_n, [Nd(HCO₂)(SO₄)(H₂O)]_n, and [Eu(HCO₂)(SO₄)(H₂O)]_n are 0.7, 0.8, 0.7, 0.5, and 0.7 times that of urea, respectively. It is particularly interesting that [Pr(HCO₂)(SO₄)(H₂O)]_n shows good two-photon absorption.

INTRODUCTION

The significant interest in the crystal engineering of chiral three-dimensional (3D) coordination frameworks reflects their structural diversity and wide-spread applications in enantioselective separation and catalysis.^{1,2} Although great efforts have been made, most of the chiral coordination compounds are discrete. Therefore, the design and synthesis of high-dimensional chiral coordination frameworks are a big challenge in both material and coordination chemistry.

According to the chiral coordination frameworks reported, two synthetic strategies were used to approach the goal. The first strategy is to employ chiral organic ligands in stereoselective synthesis.^{3–6} The second strategy is spontaneous resolution upon crystallization without chiral species.^{7–11} If there are preferential and extended homochiral connections between the neighboring chiral units, the chirality should extend to higher dimensionality, while the probability of

spontaneous resolution would be able to increase. The chirally discriminative connections may arise from coordination- and/or hydrogen-bonding interactions.⁷

Now, we are focusing our attention on building 3D chiral lanthanide sulfates without any chiral auxiliary. Compared with other transition metals, not only can the rare-earth elements adopt Ln/O radius ratios to form polyhedra with coordination of 8, 9, 10, and 12 but also the Ln–O distances are significantly longer.^{12–17} The flexibility of the polyhedral structure for rare-earth elements allows the formation of various helical chains.^{15–17} Here we report the hydrothermal synthesis and structural characterization of 10 chiral 3D framework lanthanide coordination compounds: L- and D-[Ln(HCO₂)(SO₄)(H₂O)]_n (Ln = La, Ce, Pr, Nd, and Eu), which are of

Received: October 1, 2012

Published: November 26, 2012

Table 1. Crystal Data and Structure Refinements for 1–10

	1	2	3	4	5
formula	CH ₃ EuO ₇ S	CH ₃ LaO ₇ S	CH ₃ CeO ₇ S	CH ₃ PrO ₇ S	CH ₃ NdO ₇ S
fw	311.05	298.00	299.21	300.00	303.33
T (K)	296(2)	296(2)	296(2)	296(2)	296(2)
wavelength (Å)	0.71073	0.71073	0.71073	0.71073	0.71073
cryst syst	tetragonal	tetragonal	tetragonal	tetragonal	tetragonal
space group	P ₄ ₃	P ₄ ₃	P ₄ ₃	P ₄ ₃	P ₄ ₃
a (Å)	6.9111(16)	6.9920(10)	6.9967(3)	6.9873(5)	6.9724(4)
b (Å)	6.9111(16)	6.9920(10)	6.9967(3)	6.9873(5)	6.9724(4)
c (Å)	11.604(5)	11.8201(3)	11.7780(11)	11.7373(17)	11.7007(16)
α (deg)	90	90	90	90	90
β (deg)	90	90	90	90	90
γ (deg)	90	90	90	90	90
V (Å ³)	554.2(3)	579.053(19)	576.58(6)	573.04(10)	568.82(9)
Z	4	4	4	4	4
D _c (g/m ³)	3.728	3.418	3.447	3.477	3.542
μ (mm ⁻¹)	11.672	7.718	8.237	8.846	9.474
F(000)	576	552	556	560	564
cryst size (mm ³)	0.14 × 0.14 × 0.13	0.14 × 0.14 × 0.13	0.14 × 0.14 × 0.12	0.16 × 0.14 × 0.10	0.17 × 0.13 × 0.12
θ range (deg)	2.95–25.96	2.91–25.98	2.91–25.98	2.92–25.92	2.92–25.00
limiting indices	−8 ≤ h ≤ 8, −8 ≤ k ≤ 8, −14 ≤ l ≤ 14	−5 ≤ h ≤ 8, −6 ≤ k ≤ 8, −11 ≤ l ≤ 14	−8 ≤ h ≤ 8, −8 ≤ k ≤ 8, −14 ≤ l ≤ 13	−8 ≤ h ≤ 8, −8 ≤ k ≤ 7, −14 ≤ l ≤ 14	−8 ≤ h ≤ 8, −8 ≤ k ≤ 8, −13 ≤ l ≤ 13
reflns collected	3988	2293	4247	4193	3955
indep reflns	1053	1064	1103	1109	1000
R(int)	0.0393	0.0170	0.0309	0.0170	0.0393
data/restraints/ param	1053/2/101	1064/4/101	1103/7/102	1109/7/102	1000/15/101
GOF	1.036	0.998	1.025	1.055	1.110
Flack param	−0.054(19)	0.016(15)	−0.058(15)	−0.051(18)	−0.03(4)
R1 ^a , wR2 ^b [I > 2σ(I)]	0.0191, 0.0446	0.0121, 0.0272	0.0130, 0.0317	0.0173, 0.0404	0.0225, 0.0573
R1, wR2 (all data)	0.0194, 0.0448	0.0123, 0.0273	0.0132, 0.0318	0.0174, 0.0405	0.0226, 0.0574
	6	7	8	9	10
formula	CH ₃ EuO ₇ S	CH ₃ LaO ₇ S	CH ₃ CeO ₇ S	CH ₃ PrO ₇ S	CH ₃ NdO ₇ S
fw	311.05	298.00	299.21	300.00	303.33
T (K)	296(2)	296(2)	296(2)	296(2)	296(2)
wavelength (Å)	0.71073	0.71073	0.71073	0.71073	0.71073
cryst syst	tetragonal	tetragonal	tetragonal	tetragonal	tetragonal
space group	P ₄ ₁	P ₄ ₁	P ₄ ₁	P ₄ ₁	P ₄ ₁
a (Å)	6.9130(5)	7.0078(3)	6.9951(3)	6.9876(4)	6.9706(3)
b (Å)	6.9130(5)	7.0078(3)	6.9951(3)	6.9876(4)	6.9706(3)
c (Å)	11.5956(18)	11.8399(8)	11.7739(10)	11.7374(15)	11.6921(10)
α (deg)	90	90	90	90	90
β (deg)	90	90	90	90	90
γ (deg)	90	90	90	90	90
V (Å ³)	554.15(10)	581.55(5)	576.11(6)	573.10(9)	568.11(6)
Z	4	4	4	4	4
D _c (g/m ³)	3.728	3.404	3.450	3.477	3.546
μ (mm ⁻¹)	11.674	7.686	8.243	8.845	9.486
F(000)	576	552	556	560	564
cryst size (mm ³)	0.16 × 0.14 × 0.10	0.16 × 0.13 × 0.10	0.14 × 0.12 × 0.12	0.17 × 0.17 × 0.10	0.13 × 0.13 × 0.12
θ range (deg)	2.95–25.97	3.363–26.665	2.91–25.99	2.92–25.46	2.92–25.99
limiting indices	−8 ≤ h ≤ 8, −8 ≤ k ≤ 8, −14 ≤ l ≤ 13	−8 ≤ h ≤ 8, −7 ≤ k ≤ 8, −14 ≤ l ≤ 14	−8 ≤ h ≤ 8, −4 ≤ k ≤ 8, −14 ≤ l ≤ 14	−8 ≤ h ≤ 8, −8 ≤ k ≤ 8, −14 ≤ l ≤ 14	−8 ≤ h ≤ 8, −8 ≤ k ≤ 8, −9 ≤ l ≤ 14
reflns collected	4038	4298	3147	4149	3103
indep reflns	1045	1118	1130	1063	982
R(int)	0.0348	0.0170	0.0237	0.0170	0.0216
data/restraints/ param	1045/3/101	1118/7/102	1103/7/101	1063/7/102	982/7/101
GOF	1.045	1.066	1.044	1.003	1.130
Flack param	−0.069(17)	0.003(17)	−0.027(17)	−0.01(2)	−0.025(18)

Table 1. continued

	6	7	8	9	10
R1 ^a , wR2 ^b [$I > 2\sigma(I)$]	0.0163, 0.0388	0.0151, 0.0323	0.0143, 0.0336	0.0169, 0.0414	0.0154, 0.0355
R1, wR2 (all data)	0.0164, 0.0389	0.0154, 0.0324	0.0144, 0.0337	0.0170, 0.0415	0.0155, 0.0355

^aR1 = $\sum ||F_o| - |F_c|| / \sum |F_o|$. ^bwR2 = $\sum [w(F_o^2 - F_c^2)^2] / \sum [w(F_o^2)]^{1/2}$.

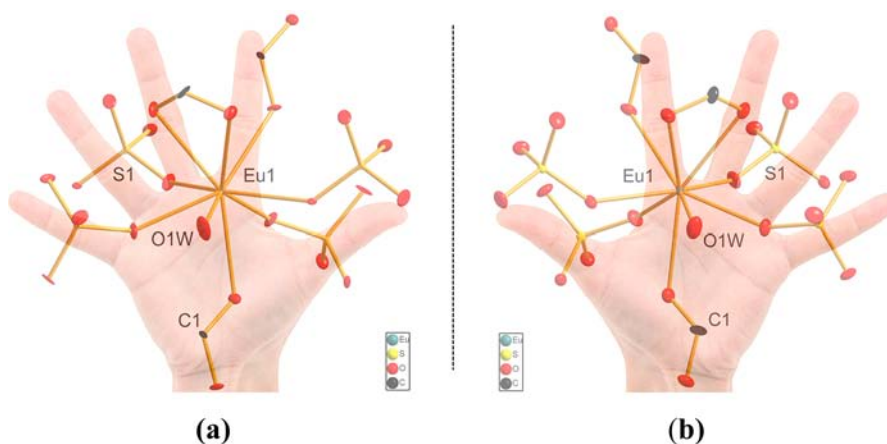


Figure 1. (a) Coordination environment of Eu³⁺ in D-[Eu(HCO₂)(SO₄)(H₂O)]_n in **6**. (b) Coordination environment of Eu³⁺ in **1**.

particular interest on the selectivity of lanthanide for symmetry and chirality. If a symmetry of P₄₃ is chosen, the chirality of the framework should be laevogyrate, while dextrogyrous chiral frameworks choose a symmetry of P₄₁.

EXPERIMENTAL SECTION

Materials and Methods. All chemicals purchased were of reagent grade and were used without further purification. IR spectra were recorded on a Nicolet Impact 410 Fourier transform infrared spectrometer using KBr pellets in the 4000–400 cm⁻¹ region. Elemental analyses of C and H were performed on a Perkin-Elmer 2400 CHN elemental analyzer. Thermogravimetric analyses (TGA) were carried out in a N₂ atmosphere on a Diamond thermogravimetric analyzer from 50 to 1100 °C with a heating rate of 10 °C/min. The solid-state emission/excitation spectra of [Ln(HCO₂)(SO₄)(H₂O)]_n were measured on a FP-6500 spectrofluorimeter equipped with a 450 W xenon lamp as the excitation source. Optical second-harmonic-generation (SHG) efficiencies were investigated by a Q-switched Nd:YAG laser (wavelength = 1064 nm and pulse width = 10 ns) at room temperature. Two-photon absorption (2PA) cross sections (δ) were obtained by using a Chameleon II femtosecond laser pulse and a Ti:95 sapphire system (680–1080 nm, 80 MHz, 140 fs). Single-crystal structure determination was performed on a Bruker SMART APEX2 CCD diffractometer at 293 K and a sealed tube X-ray source (Mo Kα radiation, λ = 0.71073 Å) operating at 50 kV and 30 mA.

Synthesis of L- and D-Eu(HCO₂)(SO₄)(H₂O) (1 and 6). A mixture of Eu₂O₃ (0.71 mmol, 0.2495 g), HCl (0.48 mmol, 0.4 mL, 36–38%), H₂O (555.56 mmol, 10 mL), sulfuric acid (3.633 mmol, 0.3633 g, 98%), N,N-dimethylformamide (DMF; 12.98 mmol, 0.9474 g), and tetramethylammonium hydroxide (0.97 mmol, 0.3533 g, 25%) was stirred for 40 min; the final pH was 2. The mixture was sealed in a 24 mL Teflon-lined autoclave and heated at 180 °C for 6 days. After being cooled to room temperature, filtered off, and washed with distilled water, colorless block crystals were obtained. Yield: 0.0952 g, 21.6% (based on Eu^{III}). Anal. Calcd for CH₃EuO₇S: C, 3.86; H, 0.97. Found: C, 3.89; H, 0.94. IR of compounds **1** and **6** (cm⁻¹): 3506 s, 3368 s, 3208 m, 1566 vs, 1346 vs, 1149 vs, 802 s, 632 s, 557 s.

Synthesis of L- and D-La(HCO₂)(SO₄)(H₂O) (2 and 7). Compounds **2** and **7** were synthesized in a manner similar to that described for **1** and **6**, except that Eu₂O₃ was replaced by La₂O₃ (0.77 mmol, 0.2510 g). Colorless block crystals of **2** and **7** were obtained.

Yield: 0.1985 g, 43.3% (based on La^{III}). Anal. Calcd for CH₃LaO₇S: C, 4.03; H, 1.01. Found: C, 3.99; H, 0.94. IR of compounds **2** and **7** (cm⁻¹): 3503 s, 3369 s, 3190 m, 1560 vs, 1375 vs, 1143 vs, 798s, 638 s, 553 s.

Synthesis of L- and D-Ce(HCO₂)(SO₄)(H₂O) (3 and 8). Compounds **3** and **8** were synthesized in a manner similar to that described for **1** and **6**, except that Eu₂O₃ was replaced by CeO₂ (1.46 mmol, 0.2506 g). Colorless block crystals of **3** and **8** were obtained. Yield: 0.0793 g, 18.2% (based on Ce^{IV}). Anal. Calcd for CH₃CeO₇S: C, 4.01; H, 1.01. Found: C, 3.89; H, 0.94. IR of compounds **3** and **8** (cm⁻¹): 3500 s, 3369 s, 3211 w, 1560 vs, 1349 vs, 1128 vs, 798 s, 626 s, 572 s.

Synthesis of L- and D-Pr(HCO₂)(SO₄)(H₂O) (4 and 9). Compounds **4** and **9** were synthesized in a manner similar to that described for **1** and **6**, except that Eu₂O₃ was replaced by Pr₂O₃ (0.76 mmol, 0.2492 g). Green block crystals of **4** and **9** were obtained. Yield: 0.2107 g, 46.5% (based on Pr^{III}). Anal. Calcd for CH₃PrO₇S: C, 4.00; H, 1.01. Found: C, 3.89; H, 0.94. IR of compounds **4** and **9** (cm⁻¹): 3497 s, 3372 s, 3199 m, 1566 vs, 1346 vs, 1137 vs, 798 s, 626 s, 566 s.

Synthesis of L- and D-Nd(HCO₂)(SO₄)(H₂O) (5 and 10). Compounds **5** and **10** were synthesized in a manner similar to that described for **1** and **6**, except that Eu₂O₃ was replaced by Nd₂O₃ (0.75 mmol, 0.2523 g). Powdery purple block crystals of **5** and **10** were obtained. Yield: 0.2351 g, 51.7% (based on Nd^{III}). Anal. Calcd for CH₃NdO₇S: C, 3.96; H, 1.00. Found: C, 3.89; H, 0.94. IR of compounds **5** and **10** (cm⁻¹): 3500 s, 3372 s, 3193 m, 1560 vs, 1346 vs, 1137 vs, 798 s, 635 s, 558 s.

X-ray Crystallography. Single-crystal X-ray diffraction data were collected on a SMART APEX2 CCD diffractometer with graphite-monochromated Mo Kα radiation (λ = 0.71073 Å) at room temperature. A total of 10 structures were solved by direct methods and refined on F² by full-matrix least-squares methods using the SHELX97 program package. All non-H atoms were refined anisotropically. The H atoms of water for 10 structures were located from a difference map, while the H atoms of the organic moieties were included in calculated positions, assigned isotropic displacement parameters, and allowed to ride on their parent atoms. A summary of the crystallographic data and structural determination for both compounds is provided in Table 1.

RESULTS AND DISCUSSION

Synthesis. Hydrothermal synthesis has recently been demonstrated to be a powerful method in the synthesis of solid-state lanthanide sulfates. During a specific hydrothermal synthesis, many factors can affect the nucleation and crystal growth of the final products, such as the type of initial reactants, starting concentrations of the reactants, pH values, solvents, reaction temperature, and time. In our case, solvents (DMF) play an important role in the formation of L- and D-[Ln(HCO₂)(SO₄)(H₂O)]_n (Ln = La, Ce, Pr, Nd, and Eu). DMF not only acts as a solvent but also decomposes to a ligand of HCOOH. We tried to add HCOOH as a reactant, but needlelike crystals of Ln(HCOO)₃ were obtained with the hexagonal unit cell ($a = b = 10.50 \text{ \AA}$ and $c = 4.01 \text{ \AA}$). Tetramethylammonium hydroxide was not included in the final product, but without it, we could not obtain chiral L- and D-[Ln(HCO₂)(SO₄)(H₂O)]_n (Ln = La, Ce, Pr, Nd, and Eu). We tried to replace Ln₂O₃ and HCl using LnCl₃·*n*H₂O; the product [Ln(HCO₂)(SO₄)(H₂O)]_n was obtained with a similar yield. When Ln₂O₃ was used as the initial reactant, [Ln(HCO₂)(SO₄)(H₂O)]_n could not be prepared without HCl (0.4 mL, 36–38%). Also we tried to change the temperature and reaction time, but the final products were still a mixture of L- and D-[Ln(HCO₂)(SO₄)(H₂O)]_n. If the reaction temperature was over 190 °C, the product yield was very low.

Crystal Structures of L-[Ln(HCO₂)(SO₄)(H₂O)]_n (1–5). A total of five L-[Ln(HCO₂)(SO₄)(H₂O)]_n (1–5) crystallize in chiral space group *P*₄₁ and keep the same topological structure. Take compound L-[Eu(HCO₂)(SO₄)(H₂O)]_n (1) as an example. The asymmetric unit of 1 contains 10 crystallographically independent non-H atoms, and all of them belong to the inorganic framework, including a Eu atom, a formyl group, a sulfate group, and one water molecule.

As shown in Figure 1b, the Eu atom is coordinated by nine O atoms from the formyl group, sulfate group, and water molecule. The structure of 1 can be described from the building units, the helical L-[Eu–O]_n chains (Figure 2), and the formyl and sulfate group fragments. As shown in Figure 2a, Eu atoms are linked by O₅ and its symmetric partners to generate a L-helical chain, while O₆ and its symmetric partners bond Eu atoms to make other L-helical [Eu–O]_n chains (Figure 2b). The central axis for both L-helical chains is a 4-fold screw axis (4₃).

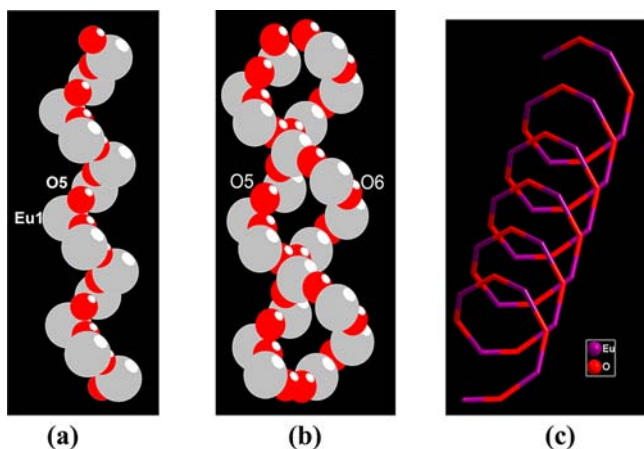


Figure 2. (a) L-Helical chain of 1 linked by O₅ and O₆. (b) Chiral interpenetrating double-helix chain of 1. (c) L-Chiral topological chain of 1.

Interestingly, adjacent L-type helical [Eu–O]_n chains are connected through O–Eu–O linkages to form chiral intertwined –[Eu–O]– double helices of left-handedness, as shown in Figure 2c. The chiral interpenetrating double helices above are particularly rare in inorganic materials, with a notable example being vanadophosphate of [(CH₃)₂NH₂]₂·K₄{V₁₀O₁₀(H₂O)(OH)₄(PO₄)₇}.^{10c} To the best of our knowledge, it is observed in the rare-earth sulfate compounds for the first time. The Flack parameter of –0.05(2) for compound 1 indicates that the absolute configurations are correct. The fragments of formyl and sulfate link the double helices to generate the chiral topological framework of 1 (Figure 3). The Eu atoms have typical geometrical parameters, with Eu–O distances of 2.315(4)–2.677(4) Å. The O–Eu–O bond angles range from 66.31(11)° to 146.38(15)°. The values are comparable with those reported earlier.^{12–15} The S atoms are tetrahedrally coordinated to four O atoms, with S–O distances in the range of 1.457(4)–1.482(3) Å, which are similar to those reported for the sulfates.^{12–16} Each S atom makes four S–O–Eu linkages through four two-bridging O atoms (S–O–Eu bridges). The S–O–S bond angles are between 108.5(2)° and 110.9(2)°, which are in agreement with 109°28', while each C atom links two double –[Eu–O]_n– helices through two three-bridging O atoms. The C–O bond distances and O–C–O angles are 1.267(4) Å and 122.4(4)°. The O_{1w} atom is attached to Eu atoms, terminal and corresponding to the water molecule. The bond distance of Eu–O(water) is 2.539(3) Å, which is involved in the strong hydrogen bond with other O atoms [O_{1w}⋯O₁ (1 – *x*, 1 – *y*, 0.5 + *z*), 2.69(2) Å; O_{1w}⋯O₂ (1 – *x*, –*y*, 0.5 + *z*), 2.78(2) Å; O_{1w}⋯O₂ (*y*, –*x*, 0.25 + *z*), 2.92(2) Å; O_{1w}⋯O₄ (1 – *x*, 1 – *y*, 0.5 + *z*), 2.95(2) Å].

Because we have not had chiral separation, L and D compounds are mixed together, and we use the mixtures to test their thermal properties. Thermal analysis shows that the total weight loss of the five mixtures occurs in two steps under N₂. Take the mixture of 1 and 6 for example. The total weight loss of 41.72% (cal. 43.41%) corresponds to the removal of H₂O, CO, and SO₃. The final residual at 1100 °C is Eu₂O₃, as shown in Figure S10 in the Supporting Information.

Crystal Structures of D-[Ln(HCO₂)(SO₄)(H₂O)]_n (6–10). When the symmetry of *P*₄₁ is selected, the chirality of the frameworks is dextrogyrous. Five chiral D-[Ln(HCO₂)(SO₄)(H₂O)]_n (6–10) crystallize in the space group *P*₄₁ and keep the same chirality. Take compound 6 as an example. As shown in Figure 1a, 6 is constructed by the building units EuO₉ polyhedra, bridging formyl and sulfate groups. As shown in Figure 4a, Eu atoms are bonded by bridging O atoms to make a D-helical chain, while other bridging O atoms bond Eu atoms to generate other D-helical [Eu–O]_n cluster chains (Figure 4b). The central axis for both D-type helical chains is a 4-fold screw axis of 4₁. Similarly, adjacent D-type helical [Eu–O]_n chains are connected through O–Eu–O linkages to form dextrogyrous chiral intertwined Eu–O double helices, as shown in Figure 4c. The Flack parameter of –0.07(2) for compound 6 indicates that the absolute configurations are correct. The bridging formyl and sulfate groups connect the double helices to perform a dextrogyrous topological framework of 6, as shown in Figure 5.

Photoluminescence Properties. The emission spectrum of mixed L- and D-[Eu(HCO₂)(SO₄)(H₂O)]_n (1 and 6), as shown in Figure 6, exhibits the characteristic transition of the Eu³⁺ ion. [Eu(HCO₂)(SO₄)(H₂O)]_n was a mixture of

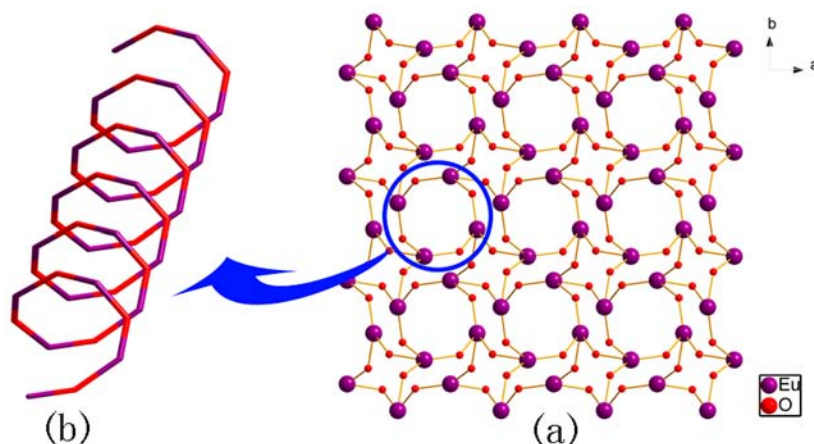


Figure 3. L-Chiral framework of **1** (S and C atoms and water molecules are removed for clarity).

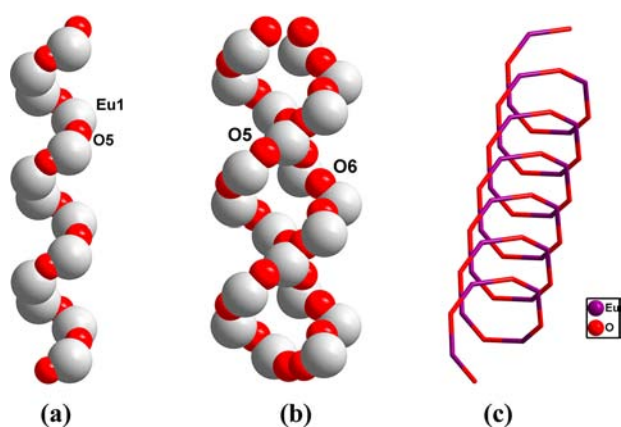


Figure 4. (a) D-Helical chain of **6** linked by O₅ and O₆. (b) Chiral interpenetrating double-helix chain of **6**. (c) D-Chiral topological chain of **6**.

compounds **1** and **6** without further chiral separation. Five bands are found that are attributed to $^5D_0 \rightarrow ^7F_J$ ($J = 0, 1, 2, 3, 4$) transitions: 586.2 nm, $^5D_0 \rightarrow ^7F_0$; 593.2 nm, $^5D_0 \rightarrow ^7F_1$; 616.0 nm, $^5D_0 \rightarrow ^7F_2$; 649.5 nm, $^5D_0 \rightarrow ^7F_3$; 693.1 nm, $^5D_0 \rightarrow ^7F_4$. It can be predicted that the five excitation bands are all of the effective energy excitation for the luminescence of Eu^{3+} .

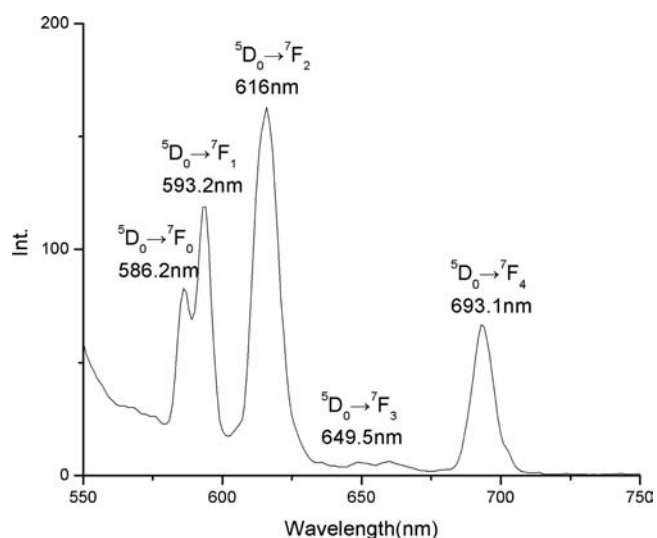


Figure 6. Solid-state emission spectra of mixed L- and D- $[\text{Eu}(\text{HCO}_2)(\text{SO}_4)(\text{H}_2\text{O})]_n$ (**1** and **6**) at room temperature.

Nonlinear-Optical (NLO) Measurement. The second-order NLO effect for the powder samples of mixed L- and D- $\text{Eu}(\text{HCO}_2)(\text{SO}_4)(\text{H}_2\text{O})$, $\text{La}(\text{HCO}_2)(\text{SO}_4)(\text{H}_2\text{O})$, $\text{Ce}(\text{HCO}_2)$ -

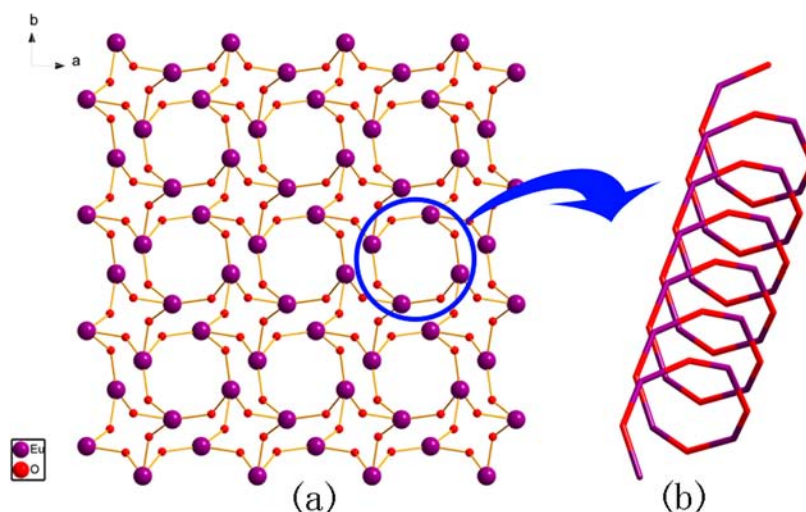


Figure 5. D-Chiral framework of **6** (S and C atoms and water molecules are removed for clarity).

(SO₄)(H₂O), Pr(HCO₂)(SO₄)(H₂O), and Nd(HCO₂)(SO₄)(H₂O) were investigated by optical SHG at room temperature. SHG intensity data were obtained by placing the powder sample in an intense fundamental beam from a Q-switched Nd:YAG laser with a wavelength 1064 nm. The output ($\lambda = 532$ nm) was first filtered to remove the multiplier and then displayed on an oscilloscope. This procedure was repeated using a standard NLO material (microcrystalline urea), and the ratio of the SHG intensity outputs was calculated. The observed SHG efficiencies are 0.7, 0.8, 0.7, 0.5, and 0.7 times that of urea for [La(HCO₂)(SO₄)(H₂O)]_n, Ce(HCO₂)(SO₄)(H₂O)]_n, [Pr(HCO₂)(SO₄)(H₂O)]_n, [Nd(HCO₂)(SO₄)(H₂O)]_n, and [Eu(HCO₂)(SO₄)(H₂O)]_n, respectively.

2PA. 2PA cross sections (δ) of a mixture of L- and D-[Pr(HCO₂)(SO₄)(H₂O)]_n were obtained by an open-aperture Z-scan technique using a femtosecond laser pulse and a Ti:95 sapphire system (680–1080 nm, 80 MHz, 140 fs). For other compounds, 2PAs were not observed. The sample was recorded as Nujol mulls between quartz plates and determined under a laser wavelength of 720 nm. Figure 7 shows the typical Z-scan

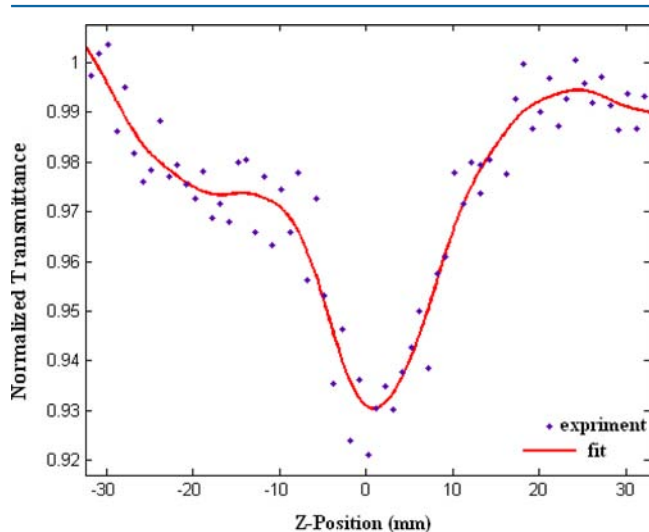


Figure 7. Z-scan data for mixed D- and L-[Pr(HCO₂)(SO₄)(H₂O)]_n in the solid state, obtained under an open-aperture configuration. The black dots are the experimental data, and the solid curve is the theoretical fit.

measurement of [Pr(HCO₂)(SO₄)(H₂O)]_n. The filled squares represent the experimental data, and the solid line is the theoretical curve modified from the following equations:¹⁸

$$T(z, s = 1) = \sum_{m=0}^{\infty} \frac{[-q_0(z)]^m}{(m+1)^{3/2}} \quad (1)$$

$$q_0(z) = \frac{\beta I_0 L_{\text{eff}}}{1+x^2} \quad (2)$$

where $x = z/z_0$, in which $z_0 = \pi\omega_0^2/\lambda$ is the diffraction length of the beam, where ω_0 is the spot size at the focus, λ is the wavelength of the beam, and z is the sample position. I_0 is the input intensity at the focus $z = 0$ and equals the input energy divided by $\pi\omega_0^2$. $L_{\text{eff}} = (1 - e^{-\alpha L})/\alpha$ is the effective length, in which α is the linear absorption coefficient and L is the sample length. By using the above equations, we obtain the nonlinear absorption coefficient β . Furthermore, the molecular 2PA cross section σ can be determined by the following relationship:

$$\sigma = h\nu\beta/N_A d \times 10^3 \quad (3)$$

where $h\nu$ is the energy of the incident photon, N_A is Avogadro's constant, and d is the concentration of the compound. The nonlinear absorption coefficient β and 2PA cross section of the compound are calculated as 0.04521 cm/GM (1 GM = 10⁻⁵⁰ cm⁴·s/photo). The nonlinear absorption coefficient and molecular 2PA cross section agree well with the values measured by an open-aperture Z-scan technique.

CONCLUSIONS

In conclusion, 10 novel chiral lanthanide coordination compounds have been synthesized by an achiral ligand. The formations of 10 chiral compounds show an interesting example of completed resolution in chirality, a progression from achiral species to chiral helical chains, to double helical chains, and finally to chiral crystals. Of particular interest, a mixture of L- and D-[Pr(HCO₂)(SO₄)(H₂O)]_n shows good NLO properties.

ASSOCIATED CONTENT

Supporting Information

X-ray crystallographic data in CIF format, IR spectra, and TGA. This material is available free of charge via the Internet at <http://pubs.acs.org>.

AUTHOR INFORMATION

Corresponding Author

*E-mail: yanxu@njut.edu.cn (Y.X.). Tel: 86-25-83587857. Fax: 86-25-83211563.

Notes

The authors declare no competing financial interest.

ACKNOWLEDGMENTS

We thank Dr. Zhang and Prof. Tian (The University of Anhui) for their help with the measurement of 2PA. This work was supported by the National Natural Science Foundation of China (Grants 20971068 and 21171093) and Jiangsu Province (Grant BK2012823).

REFERENCES

- (1) (a) Judd, D. A. J.; Nettles, H.; Nevins, N.; Snyder, J. P.; Liotta, D. C.; Tang, J.; Ermolieff, J.; Schinazi, R. F.; Hill, C. L. *J. Am. Chem. Soc.* **2001**, *123*, 886–897. (b) Müller, A.; Peters, F.; Pope, M. T.; Gatteschi, D. *Chem. Rev.* **1998**, *98*, 239–272.
- (2) Hargman, P. J.; Hargman, D.; Zubieta, J. *Angew. Chem., Int. Ed.* **1999**, *38*, 2638–2684.
- (3) (a) Kumaiga, H.; Inoue, K. *Angew. Chem., Int. Ed.* **1999**, *38*, 1601–1603. (b) Minguet, M.; Luneau, D.; Lhotel, E.; Villar, V.; Paulsen, C.; Amabilino, D. B.; Veciana, J. *Angew. Chem., Int. Ed.* **2002**, *41*, 586–589. (c) Inoue, K.; Imai, H.; Ghalsasi, P. S.; Kikuchi, K.; Ohba, M.; Okawa, H.; Yakhmi, J. V. *Angew. Chem., Int. Ed.* **2001**, *40*, 4242–4245.
- (4) Zelewskv, A.; von Knof, U. *Angew. Chem., Int. Ed.* **1999**, *38*, 302–322.
- (5) (a) Xin, F. B.; Pope, M. T. *J. Am. Chem. Soc.* **1996**, *118*, 7731–7736. (b) Long, D. L.; Kögerler, P.; Farrugia, L. J.; Cronin, L. *Chem.—Asian J.* **2006**, *1*, 352–357. (c) Long, D. L.; Burkholder, E.; Cronin, L. *Chem. Soc. Rev.* **2007**, *36*, 105–121. (d) Streb, C.; Long, D. L.; Cronin, L. *Chem. Commun.* **2007**, 471–473.
- (6) (a) Kortz, U.; Savelieff, M. G.; Ghali, F. Y. A.; Khalil, L. M.; Maalouf, S. A.; Sinno, D. I. *Angew. Chem., Int. Ed.* **2002**, *41*, 4070–4073. (b) Fang, X. K.; Anderson, T. M.; Hill, C. L. *Angew. Chem., Int.*

Ed. **2005**, *44*, 3540–3544. (c) Fang, X. K.; Anderson, T. M.; Hou, Y.; Hill, C. L. *Chem. Commun.* **2005**, 5044–5046.

(7) Gao, E. Q.; Bai, S. Q.; Wang, Z. M.; Yan, C. H. *J. Am. Chem. Soc.* **2003**, *125*, 4984.

(8) (a) Coronado, E.; Galán-Mascarós, J. R.; Gómez-García, C. J.; Martínez-Agudo, J. M. *Inorg. Chem.* **2001**, *40*, 113–120. (b) Han, S.; Manson, J. L.; Kim, J.; Miller, J. *Inorg. Chem.* **2000**, *39*, 4182–4185. (c) Sporer, C.; Wurst, K.; Amabilino, D. B.; Ruiz-Molina, D.; Kopacka, H.; Jaitner, P.; Veciana, J. *Chem. Commun.* **2002**, 2342–2343.

(9) Pérez-García, L.; Amabilino, D. B. *Chem. Soc. Rev.* **2002**, *31*, 342–356.

(10) (a) Katsuki, I.; Motoda, Y.; Sunatsuki, Y.; Matsumoto, N.; Nakashima, T.; Kojima, M. *J. Am. Chem. Soc.* **2002**, *124*, 629–640. (b) Ezuhara, T.; Endo, K.; Aoyama, Y. *J. Am. Chem. Soc.* **1999**, *121*, 3279–3283. (c) Tabellion, F. M.; Seidel, S. R.; Arif, A. M.; Stang, P. J. *Angew. Chem., Int. Ed.* **2001**, *40*, 1529. (d) Sasa, M.; Tanaka, K.; Bu, X. H.; Shiro, M.; Shionoya, M. *J. Am. Chem. Soc.* **2001**, *123*, 10750–10751.

(11) (a) Tan, H. Q.; Li, Y. G.; Zhang, Z. M.; Qin, C.; Wang, X. L.; Wang, E. B.; Su, Z. M. *J. Am. Chem. Soc.* **2007**, *129*, 10066–10067. (b) Cheetham, A. K.; Férey, G.; Loiseau, T. *Angew. Chem., Int. Ed.* **1999**, *38*, 3268–3292. (c) Zubieta, J.; O'Connor, C. J. *Science* **1993**, *259*, 1596–1599. (d) Cheetham, A. K.; Férey, G.; Loiseau, T. *Angew. Chem., Int. Ed.* **1999**, *38*, 3268–3292.

(12) (a) Wickleder, M. S. *Chem. Rev.* **2002**, *102*, 2011–2088. (b) Xing, Y.; Zhan, S.; Li, G. H.; Pang, W. Q. *Dalton Trans.* **2003**, 940–943. (c) Bataille, T.; Louer, D. J. *Mater. Chem.* **2002**, *12*, 3487–3493. (d) Dan, M.; Behera, J. N.; Rao, C. N. R. *J. Mater. Chem.* **2004**, *14*, 1257–1265.

(13) Doran, M.; Norquist, A. N.; O'Hare, D. *Chem. Commun.* **2002**, 2946–2947.

(14) (a) Wang, D.; Yu, R.; Xu, Y.; Feng, S.; Xu, R.; Kumada, N.; Kinomura, N.; Matsumura, Y.; Takanno, M. *Chem. Lett.* **2002**, *11*, 1120–1121. (b) Dolzhenkova, E. F.; Shekhovtsov, A. N.; Tolmachev, A. V.; Dubovik, M. F.; Grinyov, B. V.; Tarasov, V. A.; Baumer, V. N.; Zelenskaya, O. V. *J. Cryst. Growth* **2001**, *233*, 473–476. (c) Xing, Y.; Liu, Y. L.; Shi, Z.; Meng, H.; Pang, W. J. *Solid State Chem.* **2003**, *174*, 381–385.

(15) Xu, Y.; Ding, S.; Zheng, X. *J. Solid State Chem.* **2007**, *180*, 2020–2025.

(16) Ye, N.; Stone-Sundberg, J. L.; Hruschka, M. A.; Aka, G.; Kong, W.; Keszler, D. A. *Chem. Mater.* **2005**, *17*, 2687–2692.

(17) Perles, J.; Fortes-Revilla, C.; Puebla, E.; Iglesias, M.; Monge, M. A.; Ruiz-Valero, C.; Snejko, N. *Chem. Mater.* **2005**, *17*, 2701–2706.

(18) (a) Li, D. M.; Zhang, Q.; Wang, P.; Wu, J. Y.; Kan, Y. H.; Tian, Y. P.; Zhou, H. P.; Yang, J. X.; Tao, X. T.; Jiang, M. H. *Dalton Trans.* **2011**, *40*, 8170–8178. (b) Geethakrishnan, T.; Palanisamy, P. K. *Opt. Commun.* **2007**, *270*, 424–428.